PETROLEUM EXPLORATION AND DEVELOPMENT
Volume 50, Issue 6, December 2023
Online English edition of the Chinese language journal

Available online at www.sciencedirect.com
ScienceDirect

Cite this article as: PETROL. EXPLOR. DEVELOP., 2023, 50(6): 1269–1281.

RESEARCH PAPER

In-situ hydrocarbon formation and accumulation mechanisms of micro- and nano-scale pore-fracture in Gulong shale, Songliao Basin, NE China

WANG Xiaojun[1, 2, *], CUI Baowen[1, 2], FENG Zihui[1, 3], SHAO Hongmei[1, 3], HUO Qiuli[1, 3], ZHANG Bin[4], GAO Bo[1, 3], ZENG Huasen[1, 3]

1. National Key Laboratory of Continental Shale Oil, Daqing 163002, China;
2. PetroChina Daqing Oilfield Co., Ltd., Daqing 163002, China;
3. PetroChina Daqing Oilfield Exploration and Development Research Institute, Daqing 163712, China;
4. PetroChina Research Institute of Petroleum Exploration & Development, Beijing 100083, China

Abstract: By conducting experimental analyses, including thermal pyrolysis, micro-/nano-CT, argon-ion polishing field emission scanning electron microscopy (FE-SEM), confocal laser scanning microscopy (CLSM), and two-dimensional nuclear magnetic resonance (2D NMR), the Gulong shale oil in the Songliao Basin was investigated with respect to formation model, pore structure and accumulation mechanism. First, in the Gulong shale, there are a large number of pico-algae, nano-algae and dinoflagellates, which were formed in brackish water environment and constituted the hydrogen-rich oil source materials of shale. Second, most of the oil-generating materials of the Qingshankou Formation shale exist in the form of organo-clay complex. During organic matter thermal evolution, clay minerals had double effects of suppression and catalytic hydrogenation, which expanded shale oil window and increased light hydrocarbon yield. Third, the formation of storage space in the Gulong Shale was related to dissolution and hydrocarbon generation. With the diagenesis, micro-/nano-pores increased, pore diameter decreased and more bedding fractures appeared, which jointly gave rise to the unique reservoir with dual media (i.e. nano-scale pores and micro-scale bedding fractures) in the Gulong shale. Fourth, the micro-/nano-scale oil storage unit in the Gulong shale exhibits independent oil/gas occurrence phase, and shows that all-size pores contain oils, which occur in condensate state in micropores or in oil-gas two phase (or liquid) state in macropores/mesopores. The understanding about Gulong shale oil formation and accumulation mechanism has theoretical and practical significance for advancing continental shale oil exploration in China.

Key words: micro-/nano-scale oil storage unit; hydrocarbon occurrence phase; organo-clay complex; in-situ hydrocarbon accumulation; Gulong shale oil; Cretaceous Qingshankou Formation; Songliao Basin

Introduction

There are three types of continental shale oil, namely interlayer, hybrid, and shale [1]. The shale oil of the Cretaceous Qingshankou Formation in the Songliao Basin is a typical shale type and the first shale type that has been commercially explored in China and abroad. The first breakthrough to Qingshankou Formation shale oil was made in the Gulong sag, therefore called Gulong shale oil [2–3]. Compared with shales in other basins, Gulong shale is characterized by high shale and clay contents, and small pore size [4–7]. The shale content of Gulong shale is over 95%. Interlayers such as dolomite, shelly limestone and siltstone are thin, only a few centimeters each. The clay content is high, 25.0%–40.0% (avg. 35.6%), which is mainly illite and a little smectite at shallower layers, but missing at over 1650 m. The pore structure is complex, mainly nano–micro matrix pores and bedding fractures, and micro-fractures. Matrix pores include intergranular mineral pores, intercrystalline clay pores, organic pores, dissolution pores, etc. The pore diameter is generally 10–50 nm, and the median is 20–30 nm. The bedding fractures are 50–150 nm wide under field emission scan-

Received date: 22 Mar. 2023; **Revised date:** 20 Aug. 2023.
*** Corresponding author.** E-mail: wxiaojun@petrochina.com.cn
Foundation item: Supported by the Central Guiding Local Science and Technology Development Special Project (ZY20B13).
https://doi.org/10.1016/S1876-3804(24)60465-9

ning electron microscopy (FE-SEM).

Regarding the special type of shale, Sun et al. [8] proposed six key scientific issues, including organic matter origin and hydrocarbon generation mechanism, reservoir space structure and type, mineralogical evolution characteristics, mechanical property and reservoir stimulation mechanism, shale oil occurrence and phase, and enhancing shale oil recovery. Focusing on these issues, many studies have been conducted and lots of achievements have been gained around fine-grained sedimentary environment, hydrocarbon generation, reservoir space evolution, fracturing stimulation, and development plan. The theory of in-situ shale oil accumulation was proposed, and strongly supports the selection of sweet spots, resource assessment, fracturing treatment, and reserves submission [9–10].

Compared with other shale oil-rich basins worldwide, the formation and enrichment of Gulong shale oil are more closely related to organic matter and clay mineral evolution [11]. Controlled by the special type, there are lots of problems need to be solved to develop Gulong shale oil. Conventional hydrocarbon generation theory [12–14] shows that the origin and type of organic matter determine the hydrocarbon generation model, while clay minerals have opposite effects on hydrocarbon generation, catalysis or retardation. Gulong shale has a higher clay content whose effects on hydrocarbon generation have not been clear. With the diagenesis, pores in Gulong shale became smaller significantly, resulting in the pore throats generally less than 10 nm [6], and much smaller than the lower limit of the oil-containing pore size in the Triassic Yanchang Formation in the Ordos Basin, the Paleogene Kongdian Formation in the Bohai Bay Basin, and the Permian Lucaogou Formation in Juanggar Basin [15–18]. It is necessary to investigate how such shale oil reservoir space and flow path are constructed. Numerical simulation shows that oil in nanopores in Gulong shale has lower critical pressure, therefore, oil in small pores is in condensate state [19]. The analysis of shale oil forming condition shows that the Gulong shale oil reservoir has a complex of many independent oil-bearing micro-nano pores at different pressure and with different fluid properties [20]. However, such simulation or analysis results have not been proved in practice. In summary, as exploration and development go on, the forming and enrichment laws of shale-type shale oil will be further understood.

Taking the Qingshankou Formation shale in the Songliao Basin as a case, this paper studies the organic matter origin, shale oil formation and evolution model, reservoir pore and fracture structure and genesis, shale oil occurrence space and enrichment law through micro-nano CT, confocal laser scanning microscopy (CLSM), argon ion milling-field emission scanning electron microscopy (FE-SEM), 2D nuclear magnetic resonance spectroscopy (2D-NMR), and thermal pyrolysis of open and close systems, and proposes that Gulong shale oil is a complex of large amounts of micro-nano scale oil storage units with independent phase states. The results are not only important for the exploration of Gulong shale oil, but also scientifically significant for the theoretical understanding of terrestrial shale oil accumulation in China.

1. Overview of Gulong shale oil

The Songliao Basin covering 26×10^4 km^2 is a typical continental fault-depression lacustrine basin which is dominated by Cretaceous formations. The basin experienced two massive lake transgressions during the Late Cretaceous, resulting in the Qingshankou Fm. and the Nenjiang Fm., respectively. They are widely spread semi-deep lacustrine deposits.

Gulong shale refers to the deep-water organic-rich fine-grained laminated rock unit with certain thermal maturity and diagenesis in the terrestrial strata in the Songliao Basin [3]. Vertically, Gulong shale is mainly developed in the Upper Cretaceous Qingshankou Fm. and Nenjiang Fm., of which the Qingshankou Formation is dominant. Spatially, Gulong shale is mainly distributed in the Qijia–Gulong sag, the Sanzhao sag, and the southern Changyuan plateau, with the Qijia–Gulong sag in dominance (Fig. 1). Vertically, Gulong shale oil is mainly distributed in the first member and the lower part of the second member of the Qingshankou Fm. According to the depositional cycles, there are 9 shale oil layers (Q_1–Q_9 upward) which have been tested to have oil.

The favorable area for shale oil exploration is about 1.46×10^4 km^2, and the estimated geological resource is (100–150) $\times10^8$ t (R_o>0.75%) [9], of which the light oil zone (R_o>1.2% and oil density less than 0.83 g/cm^3) has an area of 2778 km^2. In 2021, new prediction of oil reserves was 12.68×10^8 t, and gas reserves was 3159.06×10^8 m^3 [10].

Gulong shale oil is self-sourced. Its organic matter content is high and TOC is 2%–5%. The thermally mature area is wide with R_o in the range of 0.5%–1.6%, indicating a large oil potential. Gulong shale is the primary source of conventional oil in the Daqing Changyuan plateau. In addition, Gulong shale contains abundant oil and gas, with the maximum pyrolysis free hydrocarbon content (S_1) at 15 mg/g. Well GYYP1 has produced oil and gas for more than 900 days since 2018, and the equivalent oil production is up to 1.4×10^4 t. The decline rate at the first year was only 14.5%. Many other vertical and horizontal wells also obtained good results. Ten horizontal wells drilled in the key light oil zone obtained initial oil production at 15.6–34.9 t/d, and 10–15 t [3] for a long time after one year. To date, there are more than 50 vertical wells producing oil, of which 60% are commercial. There are more than 20 horizontal wells producing oil, of which 77% are

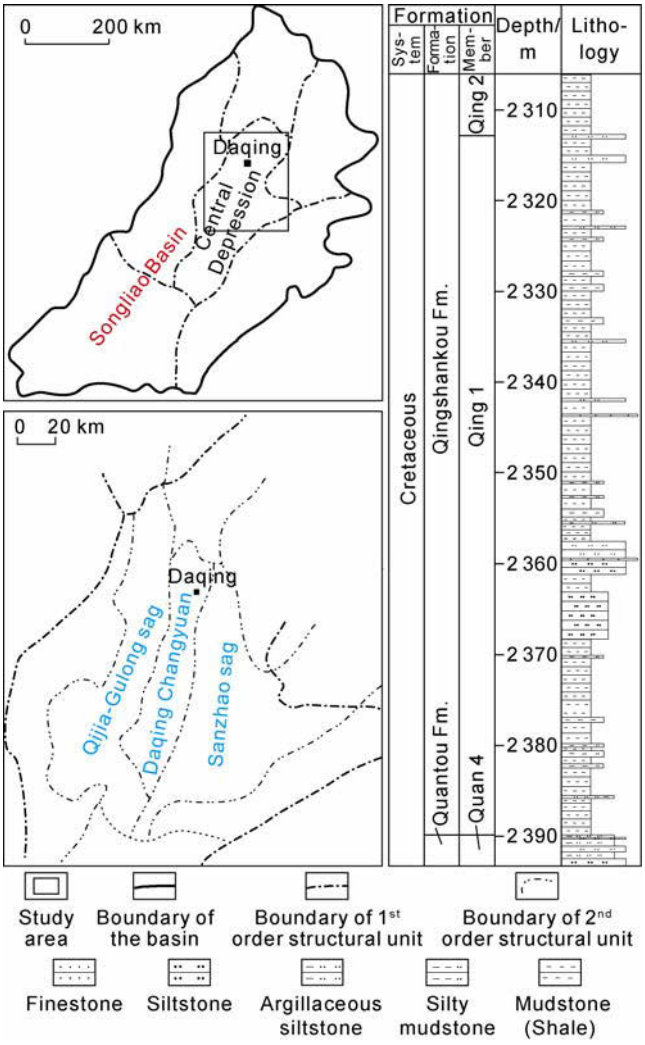

Fig. 1. Location and stratigraphic column of the study area.

commercial. The oil produced has low density of 0.74–0.82 g/cm^3, high content of light hydrocarbons (C_6–C_{14}) of 44.7%–63.8% (avg. 53.9%). The GOR is high, ranging 70–800 m^3/m^3, indicating giant exploration and development prospects.

2. Brackish water pico- and nano-algae are the main source of hydrogen-rich organic matter in Gulong shale

Compared with marine and continental shales worldwide, the Qingshankou Fm. shale has a high hydrogen index (HI) and a great oil generation potential (Fig. 1). The original hydrogen index is 600–800 mg/g (avg. 750 mg/g). The transformation ratio of kerogen is up to 78.4% [21–22]. The analysis of organic macerals shows that the proportion of alginite in organic maceral is 83%–92%, that of sporinite and cutinite is 2.7%–5.0%, and that of vitrinite and inertinite is 5.3%–12.0%. A high content of alginite is an important material guarantee for the formation of hydrogen-rich organic matter.

Based on the analyses of thin section fluorescence, organic petrology and paleontology, it is confirmed that the primary oil precursors in the Qingshankou Fm. shale are phytoplankton, including pico- and nano-algae, dinoflagellata, acritarch, and chlorophyta (Fig. 2). Their average abundance in the shale oil intervals is 56%, 26%, 15% and 3%, respectively. Among them, nano- and pico-algae are first identified in this study, and their size is 2–20 μm and 0.2–2.0 μm, respectively, and their abundance decreases upward. According to references [23–24], the algae are the smallest class of photosynthetic autotrophs discovered to

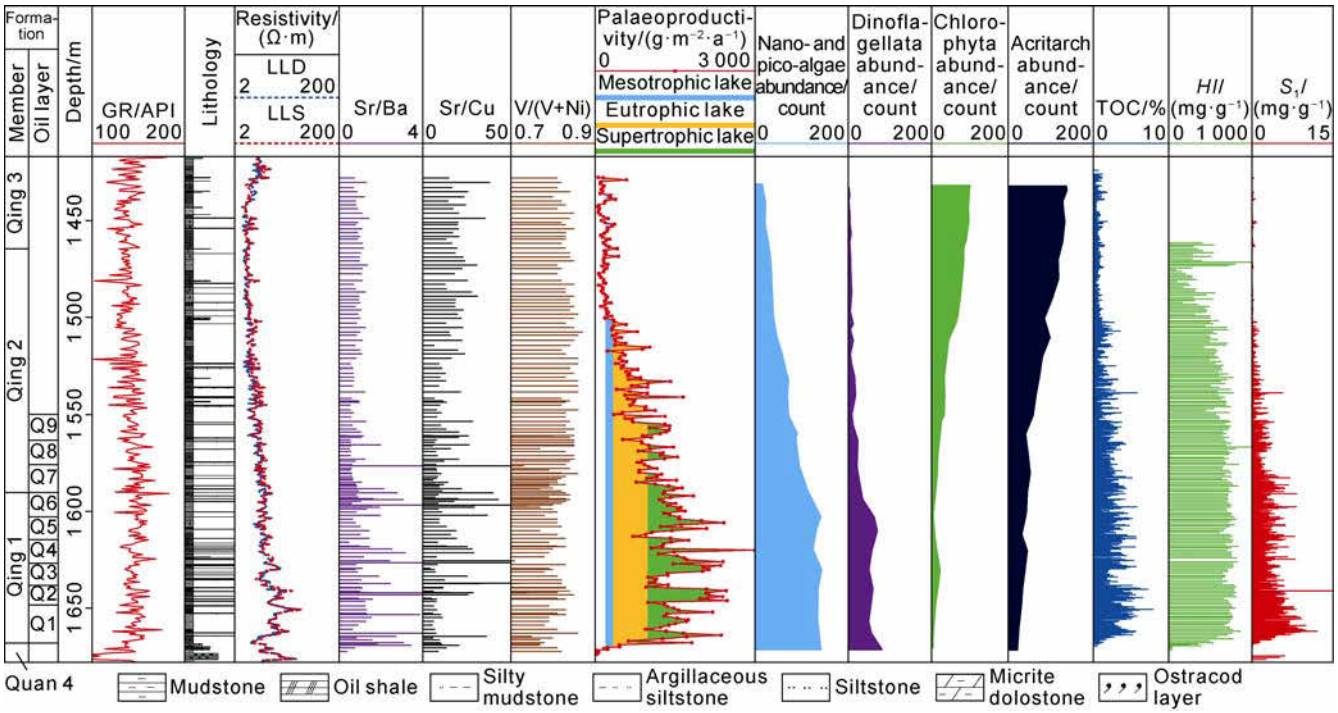

Fig. 2. Brackish water nano- and pico-algae and geochemical parameters in Qingshankou Formation shale.

date, and an important contributor to the biomass and productivity in modern marine and salt lake ecosystems.

At the early depositional stage, the Qingshankou Fm. may have been affected by marine transgression [25–26], which, on the one hand, brought massive nutrients to the lake, causing algae to boom in the ancient lake, especially the thriving of nano- and pico-algae (Fig. 2), providing material sources for the formation of the shale with high TOC and HI in the lower part of Qingshankou Fm., and on the other hand, made the salinity of the ancient lake rise, resulting in salinity stratification in the water and a strong reducing environment, providing favorable conditions for the preservation of hydrogen-rich organic matter. The massive enrichment of organic matter with abundant alginite and the excellent preservation conditions in Gulong shale laid a material foundation for the large-scale formation of shale oil.

3. Interaction between hydrogen-rich organic matter and clay minerals extends oil window and increases light hydrocarbon yield

The activation energy for hydrocarbon generation can be measured by open system pyrolysis that was conducted in a Rock-Eval [26–27]. In order to determine the influence of different types of clay minerals on hydrocarbon generation, four comparative experiments of kerogen, kerogen + smectite, kerogen + illite and kerogen + chlorite were conducted, respectively, in this study. According to the whole-rock mineral composition and TOC, the mass ratio of kerogen to clay mineral is 1 to 4. The pyrolysis experiment results show that the weighted average activation energy required by hydrocarbon generation from kerogen is 209.8 kJ/mol, which is less than the activation energy of the mixture of kerogen and clay. The weighted average activation energy required by hydrocarbon generation from the mixture of kerogen + smectite is the maximum, 211.79 kJ/mol, followed by the mixture of kerogen + chlorite, 211.19 kJ/mol, and the last kerogen + illite, 210.29 kJ/mol. The cause for the phenomenon above is the bonding interaction, namely hydrogen bond, ion dipole force, cation exchange, and Van der Waals force, between clay minerals and organic matter [28–29], which increase the activation energy for kerogen decomposition and slow the process of organic matter cracking. Clay minerals, especially smectite, have an obvious inhibitory effect on hydrocarbon generation from organic matter.

In order to quantitatively determine the hydrocarbon production at different mature stages, pyrolysis experiments on kerogen and whole rock (i.e., kerogen + clay minerals) were carried out respectively. The clay mineral composition of the core sample is 35% smectite, 23% illite, 11% kaolinite, and 13% chlorite. The experiment was conducted in a proprietary close pyrolysis system with capsular vessels. As shown in Fig. 3, the transformation ratio of the kerogen sample is higher than that of the whole rock sample when R_o is 0.5%–1.5%. According to the evolution stage of organic matter, the kerogen sample reaches its hydrocarbon generation peak when R_o is 0.8%, and the oil window corresponds to R_o in the range of 0.5%–1.3%; the whole rock sample reaches its hydrogen generation peak when R_o is 1.0% and the oil window corresponds to R_o in the range of 0.7%–1.6%. This indicates that if there are clay minerals, the thermal maturity should be higher and the oil window will extend, which is in accordance with the results of open system pyrolysis. It is worth noting that although the organic matter in the whole-rock sample reaches its peak oil generation late, the oil yield increases significantly. The amount of oil generated from the kerogen sample is only 22 mg/g (after being converted to a whole rock sample), but that generated from the whole rock sample is 32 mg/g, indicating that clay minerals can increase hydrocarbon yield.

In order to investigate the effects of clay minerals on hydrocarbon composition, we installed a proprietary pyrolysis device in front of a gas chromatograph, so that rock pyrolysis products directly entered the gas chromatograph. As shown in Fig. 4, light hydrocarbon (C_6–C_{14}) and heavy hydrocarbon (C_{14+}) yielded from a kerogen sample are similar, both about 36%, and gaseous hydrocarbon (C_1–C_5) is 28%. From the mixture of kerogen and smectite, light hydrocarbon increases to 46%, heavy hydrocarbon decreases to 28%, and gaseous hydrocarbons is 26%, indicating that smectite hydrogenation is significant in organic matter cracking. From the mixture of kerogen and illite (or chlorite), light hydrocarbon increases not as

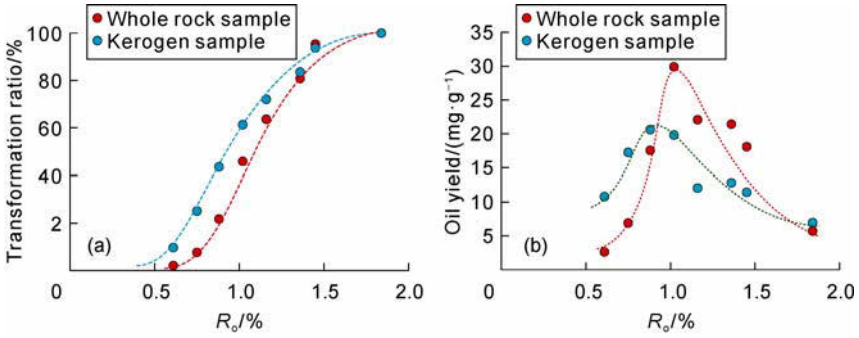

Fig. 3. Transformation ratio and oil yield vs. R_o in a closed pyrolysis system.

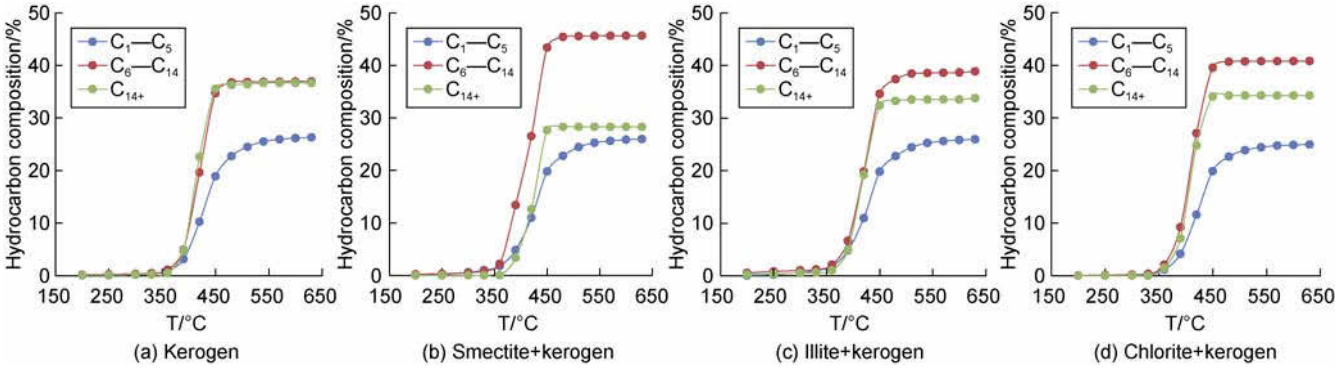

Fig. 4. Hydrocarbon composition generated from different samples in an open pyrolysis system.

high as that from the mixture of kerogen + smectite, but both (39% for illite and 41% for chlorite) higher than that from the pure kerogen sample. It is proven that the involvement of clay minerals in organic matter cracking can increase not only the total hydrocarbon yield, but also the content of light hydrocarbon. The main mechanism is that the metal hydrated ions existing in clay mineral inter-layers can provide additional hydrogen sources for oil cracking and reduce the disproportionation degree of crude oil cracking reaction [28–29], that is to inhibit the direct cracking of long-chain hydrocarbons into gas, thus increasing the content of light hydrocarbons in the final product.

4. Main accumulation space for shale oil is controlled by hydrocarbon generation and dissolution

Gulong shale has a high content of clay minerals whose particle size is at mud level. With the increase of burial depth and enhancement of diagenesis, primary intergranular pores and inter-crystalline pores decrease rapidly [30]. The analysis results of FE-SEM and energy dispersive spectroscopy (EDS) show that the formation of oil accumulation space for moderate to high mature Gulong shale oil is mainly related to hydrocarbon generation and dissolution (Fig. 5).

With the increase of thermal maturity, a large number of organic pores are formed in clay-rich shale. Conventional organic pores generally refer to the void inside organic matter, formed in solid bitumen due to thermal cracking of retained oil in intergranular pores or dissolution pores, and gas escaping at high mature stage. These organic pores are usually circular or oval with larger diameters [31–32]. In this study, FE-SEM observation of more than 80 samples from 10 wells found that Gulong shale has a few organic pores of this kind, instead most organic pores are the result of thermal evolution of organo-clay complex and related to volume shrinkage caused by

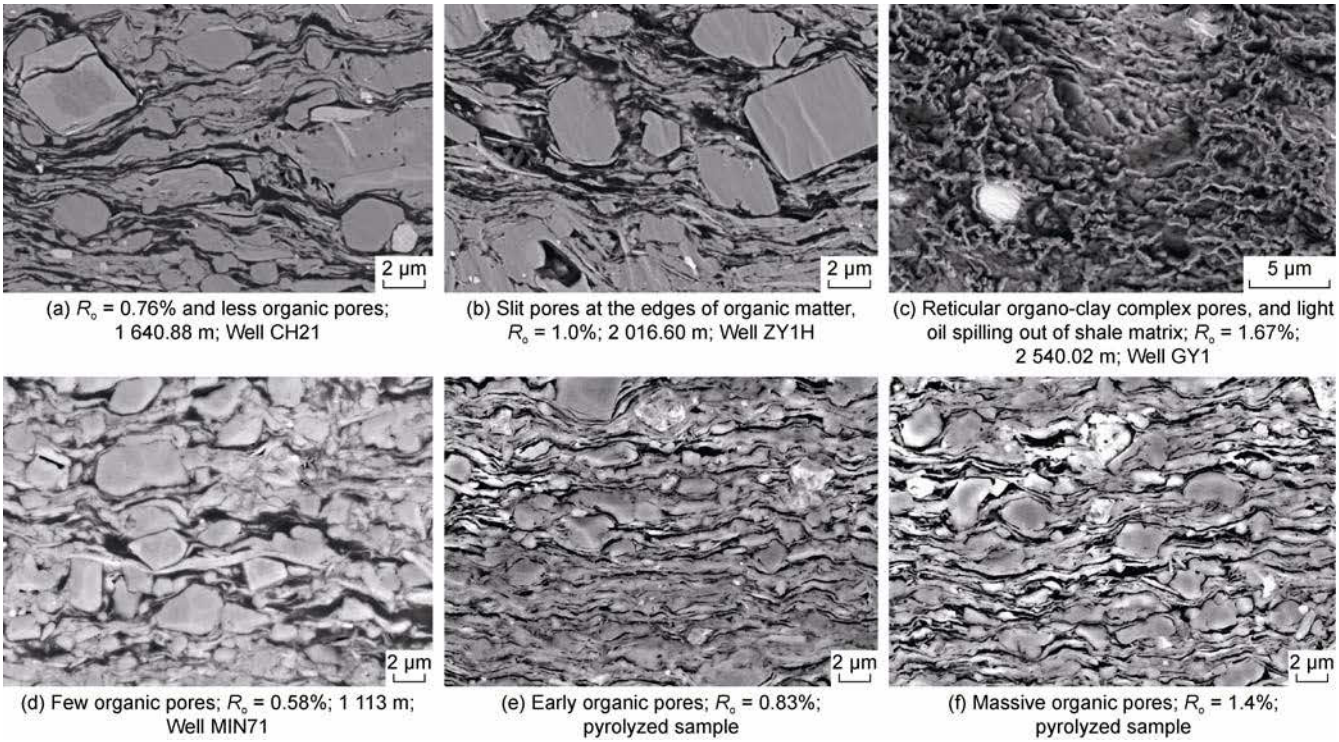

Fig. 5. Micro-characteristics of organic pores in Gulong shale with different maturity.

hydrocarbon generation. It is suggested that hydrocarbon generation is concurrent with reservoir space formation. Comparative analysis of shale samples with different maturity degrees shows that a large amount of lamalginite are distributed along bedding and a few organic pores are present in immature to low mature shales (Fig. 5a); in moderately mature shales, slit pores appear at the edges of organic matter (Fig. 5b); and in high mature shales, the number of pores at the edges of organic matter increases significantly, and a large number of reticular pores appear in organo-clay complex (Fig. 5c). This indicates that the formation of organic pores is related to the thermal evolution of organic matter.

In order to verify the formation mechanism of organic pores in Gulong shale, a low mature shale sample from Well Min71 (R_o 0.58%) was selected for pyrolysis experiment to observe the formation process of organic pores with hydrocarbon generation (Fig. 5d–5f). The results show that organic pores are undeveloped in the original sample, with the surface porosity of only 0.3% (Fig. 5d); when the temperature reaches 300 °C and the corresponding R_o value reaches 0.83%, lamalginite shrink due to hydrocarbon generation, forming slit organic pores distributed along bedding, with the surface porosity up to 5.1% (Fig. 5e); when the temperature reaches 400 °C and the corresponding R_o value is 1.4%, organic pores are developed in large quantities, with the surface porosity up to 14.5%. The experiment results prove that in the process of diagenesis, especially at mature and high-mature stages, the volume shrinkage of organic matter can form a large number of spongy or bubble organic pores and fractures. At moderate to high-mature stages of Gulong shale, influenced by the massive formation of organic pores, the total porosity shows a significant positive correlation with TOC [33].

In addition to the development of organic pores, a large number of secondary pores formed due to mineral dissolution can also be seen in Gulong shale. The EDS analysis results show that the dissolved minerals are siderite, potassium feldspar, plagioclase feldspar, etc. Dissolution pores are generally induced by organic acids formed during conversion of organic matter to oil and gas on unstable minerals in shale [34]; therefore, the development of these pores is usually related to the thermal evolution of organic matter. At immature to low-mature stage, organic matter has not started massive hydrocarbon generation yet, the content of organic acid and other acid fluids is low, and dissolution pores in shale are less than 10%, and poorly connected. At mature stage, massive organic acids promote dissolution of feldspar, carbonate, and other minerals, leaving a large number of dissolution pores. In this stage, some minerals are completely dissolved to form mold pores and the proportion of dissolution pores is up to over half of total pores, and pore connectivity becomes good. At high mature stage, the content of organic acids in shale decreases, and some particle dissolution pores are filled with neogenic minerals, such as quartz and chlorite, at the time they formed. The proportion of dissolution pores is less than 20%.

Based on a large number of measured data, porosity, pore type and pore structure evolution models are established for Gulong shale (Fig. 6). The porosity shows a trend of decreasing first and then increasing with burial depth. At high mature stage, the total porosity can be up to 15%, and the effective porosity can be up to 12%, in contrast with conventional understanding that reservoir porosity gradually decreases with burial depth. At the A1 stage of middle diagenesis, the porosity decreases with burial depth, and the pores are mainly intergranular pores, showing that intergranular pores gradually decrease with the increase of burial depth due to mechanical compaction. At the A2 stage of middle diagenesis, the porosity increases and pores are almost dissolution pores and organic pores, resulting in increasing reservoir space. At the B stage of middle diagenesis, the porosity increases further. Although the number of dissolution pores decreases, the number of organic pores increases significantly, up to 70%, so that organic pores provide the primary space for oil accumulation. The nitrogen adsorption experiment results show that the pore volume of Gulong shale increases slightly from stages A1 to B of the middle diagenesis, but the average pore radius shows a decreasing trend, from 15 nm to ca. 5 nm, indicating that organic pores are dominated by small pores. The results of high-pressure mercury intrusion analysis show that the maximum and the average pore throat radius of Gulong shale at the B stage of the middle diagenesis both have an increasing trend, which is different from the conclusion of the nitrogen adsorption experiment. The possible reason is that a large number of bedding fractures produced at the B stage increase the pore throat radius of the bulk samples used in the high-pressure mercury intrusion analysis, but have little effect on the powdered samples in the nitrogen adsorption analysis.

5. Nano-pores and micro-bedding fractures contribute to the reservoir space in Gulong shale

Based on helium porosity, a full-scale pore size distribution characterization method for shale reservoir was established by combination of nitrogen adsorption, high-pressure mercury intrusion, FE-SEM and CT techniques. The number of pores in different size intervals is determined as follows: for the pores larger than 1000 nm, both porosity and pore size distribution are determined by CT; for the pores less than 128 nm, the porosity is measured by high-pressure mercury intrusion experiment, and the pore size distribution is determined by

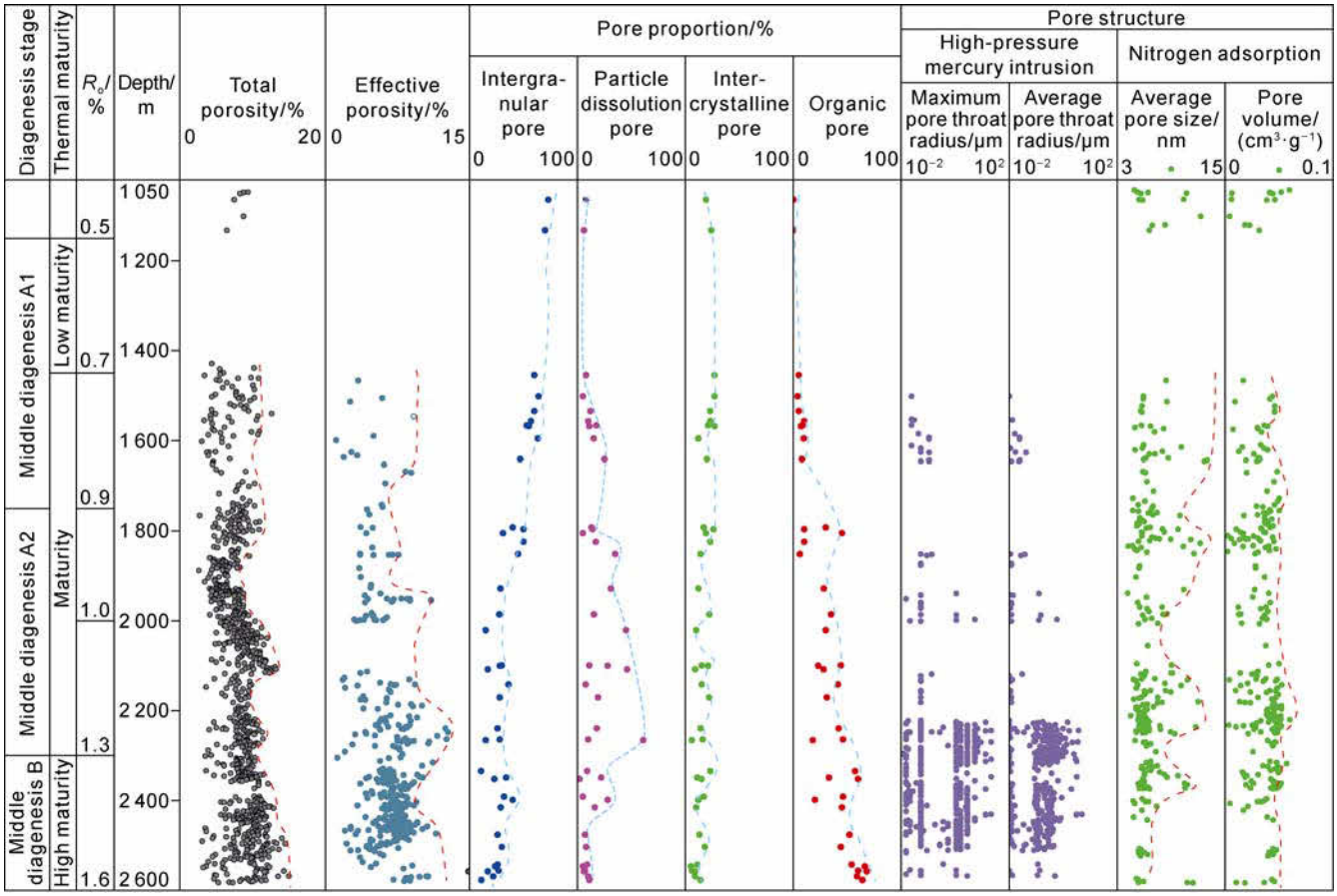

Fig. 6. Pore types and evolution with diagenesis in Gulong shale.

considering nitrogen adsorption analysis; the porosity of pores between 128 and 1000 nm is that the total porosity minus the porosity of the pores larger than 1000 nm and those smaller than 128 nm, and the pore size distribution is determined by FE-EM analysis by assuming the maximum sphere algorithm. The experimental results of all pore size intervals are normalized to get the full-scale pore size distribution.

The result shows that pore size distribution of Gulong shale with different maturities changes from large to small and from multiple peaks to single peaks with increasing maturity (Fig. 7). The maturity of the shale sample from Well CH21 is low (R_o=0.78%), and the total porosity is 4.1%. The pore size distribution shows a roughly tri-peak pattern, with main peaks at 8–32 nm, 256–512 nm and greater than 5000 nm, respectively. The porosity at the three peaks is 0.7%, 1.0%, and 0.5%, respectively, indicating coexistence of nano-pores and micro-pores. The maturity of the shale sample from Well GY2HC increases (R_o=1.37%) and the total porosity is 9.2%. The pore size distribution shows a roughly bi-peak pattern, with main peaks at 2 nm to 8 nm and 256–512 nm, respectively. The porosity at two peaks is 2.4% and 1.8%, respectively, indicating the domination of nano-pores. The maturity of the shale sample from Well GY1 is high (R_o=1.61%), and the total porosity is 10.5%. The pore size distribution shows a single peak pattern, with main peak at 2 nm to 8 nm and porosity of 3.4%. The contribution of pores smaller than 50 nm to the total porosity is over 65%, indicating that mesopores and micropores become the primary space for oil in Gulong shale. The pore diameter of Gulong shale is far smaller than that of other continental shale oil reservoirs discovered in China (mainly 80–200 nm) [35], and smaller than that of marine shale oil reservoirs (mainly 80–100 nm) [36].

The analysis results of micro-CT (a 2-cm-long sample with fracture width resolution greater than 7 μm) and nano-CT (a 2-mm-long sample with fracture width resolution of 0.7–7.0 μm) of Gulong shale show that bedding fractures are abundant and increase with thermal maturity (Table 1). When R_o is less than 1.0%, there are fewer bedding fractures, and micro-pores dominate, but nano-pores are not developed. For example, the micro-CT analysis of shale samples from wells CY6801, CH21 and ZY1 shows that the bedding fractures are 12.78–38.07 μm wide (avg. 26.47 μm), the fracture spacing is 2.3–11.31 mm (avg. 4.82 mm) and the corresponding porosity is 0.25%–3.45%. Most shale samples have fracture porosity less than 1.0%, except those affected by natural fractures. The nano-CT analysis shows that there are sparse bedding fractures in most shale samples, the visible fractures are 2.05–4.12 μm wide and the fracture porosity is only 0.05%–0.38%. When R_o vlaue larger than 1.0%, micro-CT and nano-CT analysis results show that both the number of

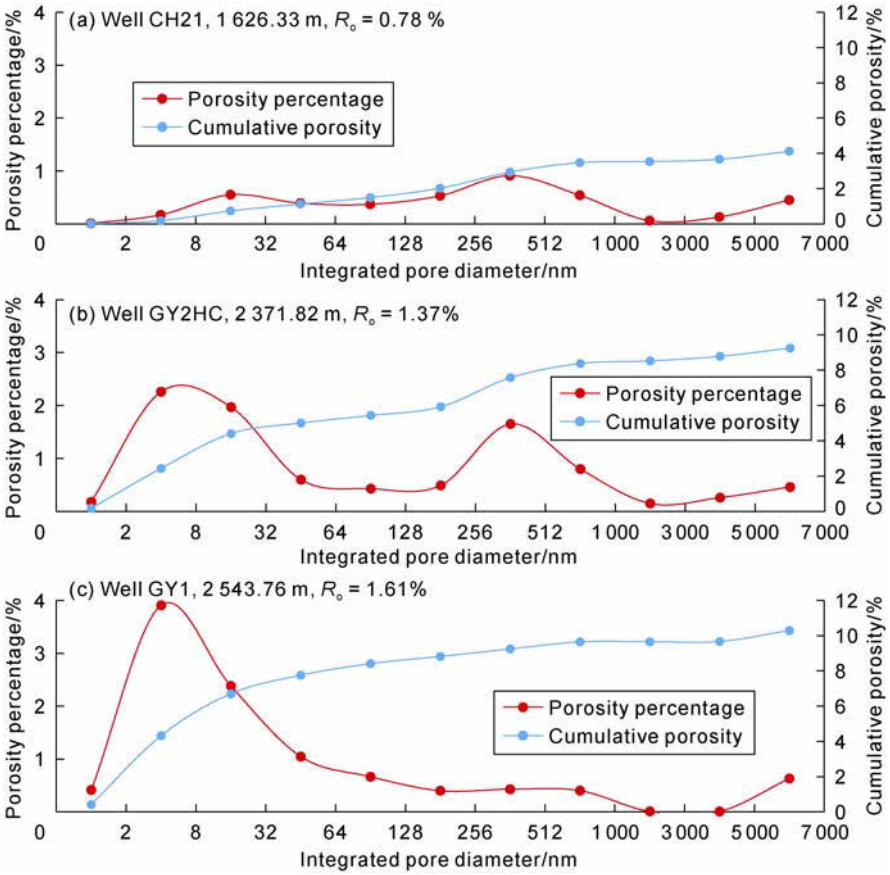

Fig. 7. Full-scale pore size distribution derived from integrated methods in Gulong shale.

Table 1. Micro-CT and nano-CT analysis of Gulong shale

Well No.	Well depth/m	R_o/ %	A 2-cm-long sample with fracture width larger than 7 μm			A 2-mm-long sample with fracture width of 0.7–7.0 μm		
			Average fracture width/μm	Average fracture spacing/mm	Porosity/ %	Average fracture width/μm	Average fracture spacing/mm	Porosity/ %
CY6801	1080.37	0.55	28.70	5.04	1.00	3.14		0.38
CY6801	1132.12	0.58	33.80	11.31	0.45			
CH21	1602.33	0.76	38.07	5.54	1.33			
CH21	1640.88	0.80	36.52		0.45			
ZY1	2032.10	0.95	16.64	2.30	0.31			
ZY1	2036.59	0.96	12.78	4.19	0.25	4.12		0.15
ZY1	2038.60	0.96	36.90	2.97	3.45	2.05		0.05
ZY1	2039.60	0.96	15.23	2.54	0.56			
ZY1	2041.60	0.99	13.48	4.71	0.28			
ZY1	2042.60	0.99	32.67		0.78			
GY3HC	2461.70	1.39	29.40	2.22	1.32	2.67	0.32	0.83
GY3HC	2476.93	1.44	38.18	2.55	1.61	2.46	0.35	0.71
GY8HC	2459.10	1.44	29.02	2.69	1.08	2.69	0.54	0.55
GY8HC	2467.80	1.46	22.70	2.61	1.07	3.15	0.42	0.94
GY1	2454.19	1.53	41.98	5.22	1.78	3.05	0.33	0.57
GY1	2497.51	1.58	32.16	3.71	1.17	3.13	0.34	0.85

bedding fractures and fracture width increase significantly. For example, the micro-CT analysis of the shale samples from Wells GY3HC, GY8HC and GY1 shows that the width of the bedding fractures ranges from 22.7 μm to 41.98 μm (avg. 32.24 μm), the fracture spacing ranges from 2.22 mm to 5.22 mm (avg. 3.16 mm), and the fracture porosity ranges from 1.08% to 1.78%. The nano-CT analysis shows the width of the bedding fractures is 2.46–3.15 μm (avg. 2.85 μm), the fracture spacing is 0.32–0.54 mm (avg. 0.38mm), and the average bedding fracture density is 2631 fractures/m. The increase in bedding fracture width and density with increasing maturity not only provides new accumulation space for Gulong shale oil (dual-porosity media, i.e., nano-pores and micro-bedding fractures), but also provides a key factor for the increase of horizontal permeability. Air permeability test results show that the vertical permeability is $(0.001–0.010)\times10^{-3}$ μm² (avg. 0.0075×10^{-3} μm²), and the horizontal permeability is $(0.01–0.45)\times10^{-3}$ μm² (avg. 0.15×10^{-3} μm²). The horizontal permeability is 20 times the vertical permeability, mainly depending on the contribution of bedding fractures.

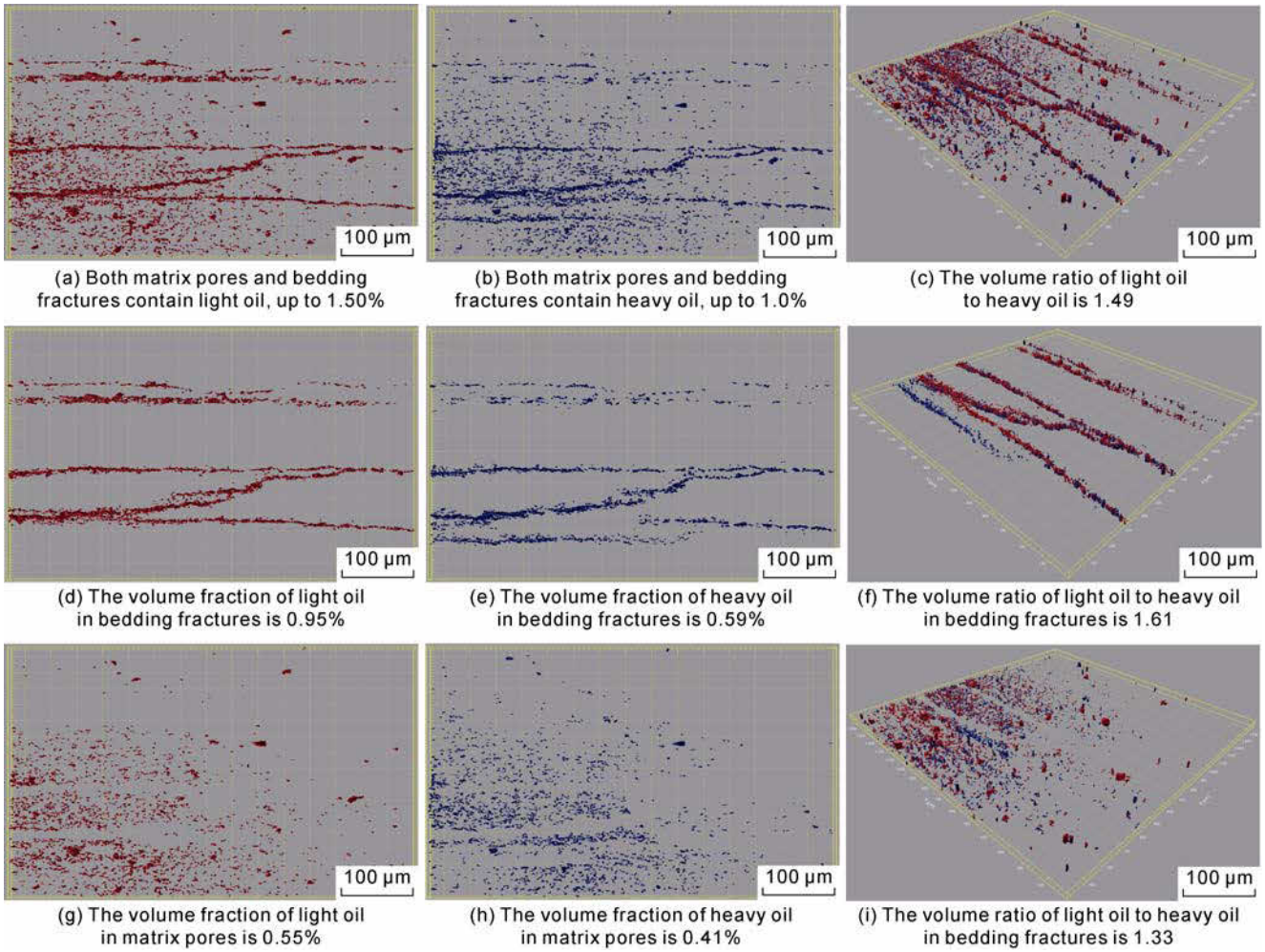

Fig. 8. CLSM images of Gulong shale oil (Shale; 1851.23 m; Well ZH2911).

The CLSM analysis results (Fig. 8) show that bedding fractures are not only oil accumulation space, but also important paths for oil migration and recovery. Both bedding fractures and matrix pores in the shale sample from Well ZH2911 (R_o=0.9%) contain oil, and the total oil content is 2.5%, including 1.5% light hydrocarbon and 1.0% heavy hydrocarbon (i.e., the ratio of light to heavy hydrocarbons is 1.5). The oil content in bedding fractures is 1.54%, in which light hydrocarbon accounts for 0.95%, and heavy hydrocarbon 0.59%, with the light-to-heavy ratio at 1.61, indicating that the oil is lighter. The oil content in matrix pores is 0.96%, in which light hydrocarbon accounts for 0.55%, and heavy hydrocarbon 0.41%, with the light-to-heavy ratio at 1.33, indicating that the oil is heavier. The shale oil in bedding fractures is significantly lighter than that in matrix pores, indicating that minor migration of shale oil occurs from matrix pores to bedding fractures. It is the micro-scale bedding fractures that connect nano-pores in shale matrix, forming a nano- and micro-scale dual-porosity media that enables the production of Gulong shale oil from most pores smaller than 50 nm.

6. Gulong shale oil is a complex of numerous micro- and nano-scale oil accumulation units with independent phase states

FE-SEM analysis of Gulong shale (Fig. 9) reveals that various pores such as organic pores, intergranular pores, inter-crystalline pores, and bedding fractures, contain oil in free, film, or impregnating states. It is suggested that shale oil occurs in various states in various types of pores. The fact that bedding fractures contain free oil suggests that they not only have accumulation significance for shale oil, but also play a key role in connecting various types of micro-pores and nano-pores and providing paths for oil migration. It should be noted that in all types of oil-bearing pores, the minimum size of detectable inter-crystalline pores is 5 nm, suggesting that all pores larger than 5 nm may contain oil. This finding breaks the old understanding that the lower limit of oil-bearing pores for tight oil is larger than 20 nm [36].

Frozen and pressure-preserved Gulong shale cores are in the original underground oil-bearing state. After unfrozen in a close environment (lasting about 20 min), 2D

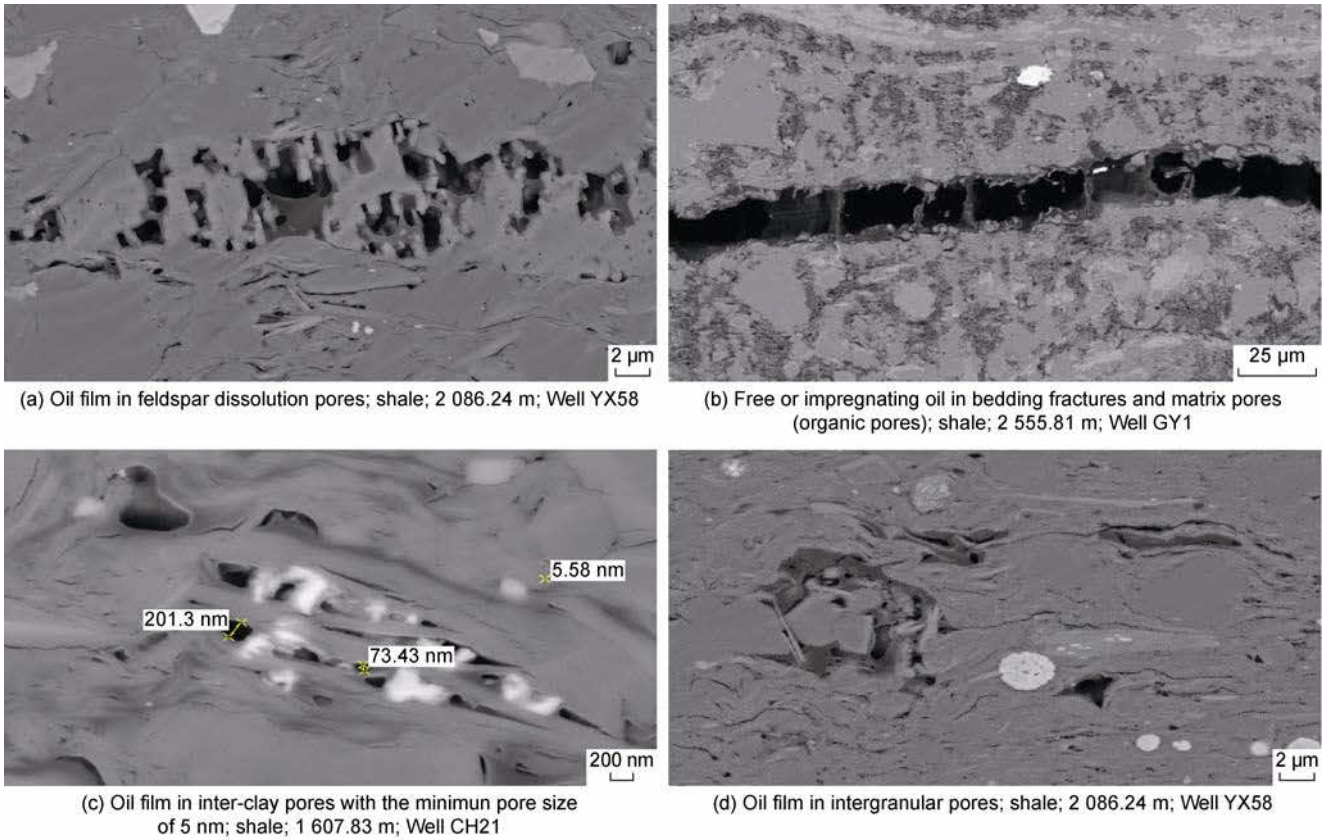

(a) Oil film in feldspar dissolution pores; shale; 2 086.24 m; Well YX58

(b) Free or impregnating oil in bedding fractures and matrix pores (organic pores); shale; 2 555.81 m; Well GY1

(c) Oil film in inter-clay pores with the minimun pore size of 5 nm; shale; 1 607.83 m; Well CH21

(d) Oil film in intergranular pores; shale; 2 086.24 m; Well YX58

Fig. 9. Occurrence states shown on the FE-SEM images of Gulong shale oil.

NMR experiment was performed on the cores to determine the original oil content. Then they were extracted by chloroform for 7 d to remove residual oil, and analyzed by 2D NMR again. By comparing the 2D NMR results before and after extraction, oil distribution in pores of different sizes was determined. The division of oil and water zones on 2D NMR T_1-T_2 map were based on references [37–38], and the relationship between relaxation time and pore size was established by comparing with high-pressure mercury intrusion results. The experiment results (Fig. 10) show multi-peak distribution of shale oil in pores of different sizes. The pores having oil in the shale sample from Well GY2HC (R_o=1.37%) ranges from 3 nm to 5000 nm, and oil almost in 20–400 nm pores. The distribution of oil-bearing pores exhibits a tri-peak pattern, with 3–10 nm, 20–60 nm, and 60–400 nm as peaks. The oil-bearing pores in the shale sample from Well GY1 (R_o=1.67%) are 4–200 nm, and the general distribution exhibits a bi-peak pattern, with 3–10 nm and 20–60 nm as peaks. With the increase of maturity, shale oil tends to accumulate in small pores. From Well GY2HC to Well GY1, the amount of oil in pores of 60–400 nm decreases, while the amount of oil in pores of 3–10 nm increases significantly. The trend of oil enrichment toward small pores in Gulong shale is due to the fact that with increasing maturity, a large number of nano-scale organic pores appear in organo-clay complex and store oil and gas there, rather than oil migrating from large pores to small pores. Oil accumulating in 3–10 nm pores further confirms that the in-situ generation and accumulation characteristic of Gulong shale oil [20].

After the original oil content was determined, the frozen and pressure-preserved core samples were exposed for 12h under indoor conditions before conducting 2D NMR analysis, in order to observe shale oil loss driven by original formation energy. The results show that the oil content in 2–10 nm pores in the shale sample from Well GY18 is about 5% in the original underground state, but it completely disappeared under aboveground natural conditions, and the loss is nearly 100% and very quick (Fig. 11). The oil content in pores of 20–400 nm is more than 90% in the underground state, and this part of oil was lost by 29.2% naturally, indicating a strong oil retention effect and a slow oil loss rate. Oil in pores larger than 400 nm accounts for less than 5% in the underground state, but 94.8% was lost after being exposed, probably due to larger pore sizes, indicating fast oil loss. Assuming oil in different pores have identical composition, small pores have a larger specific surface area and adsorption, leading to lower oil fluidity and evaporability than in larger pores. It is suggested that oil phase state is affected by nano-confinement effect [39], which significantly decreases the critical pressure and temperature of the fluid in nanopores. Oil in pores less than 10 nm has lower critical pressure and temperature, so it is condensate or gaseous at reservoir pressure and temperature. Oil in larger pores

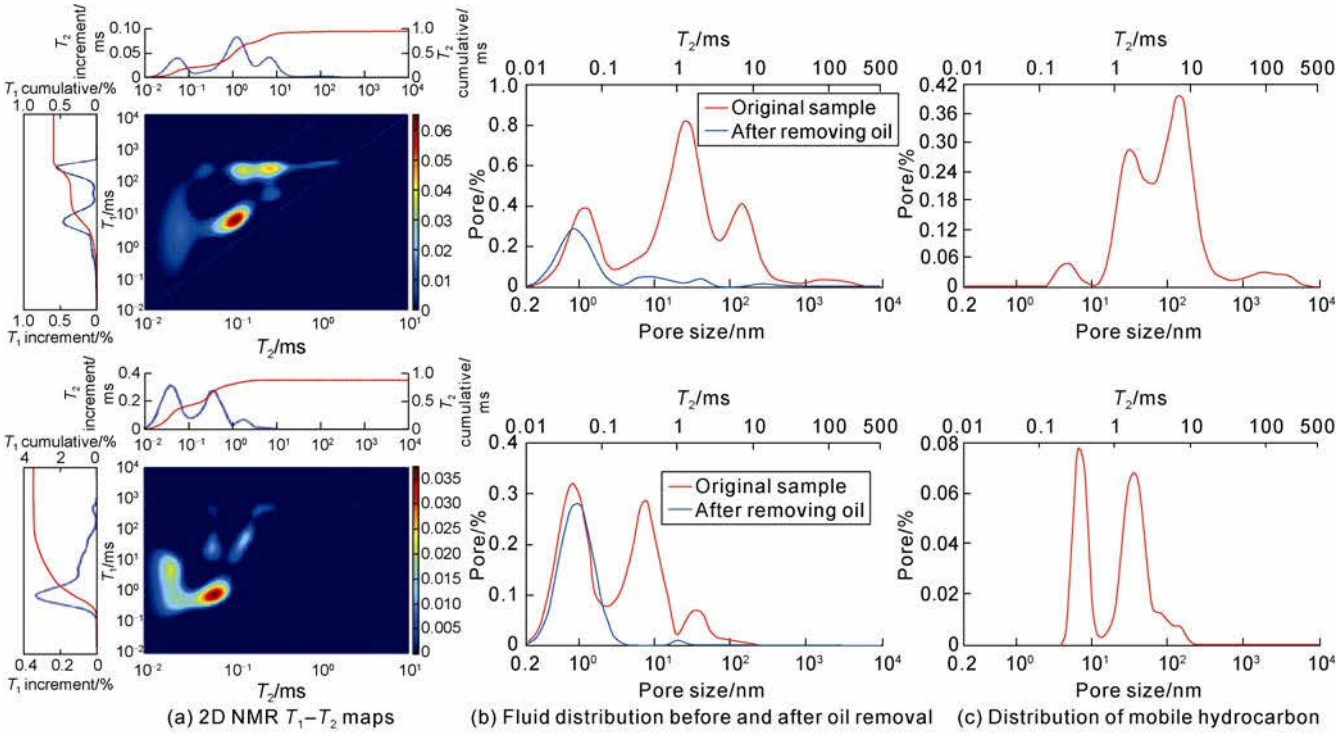

Fig. 10. 2D NMR analysis results of frozen and pressure-preserved cores before and after oil removal (*top*: Well GY2HC, 2346.09 m; *bottom*: Well GY1, 2568.82 m); T_1—longitudinal relaxation time; T_2—transverse relaxation time).

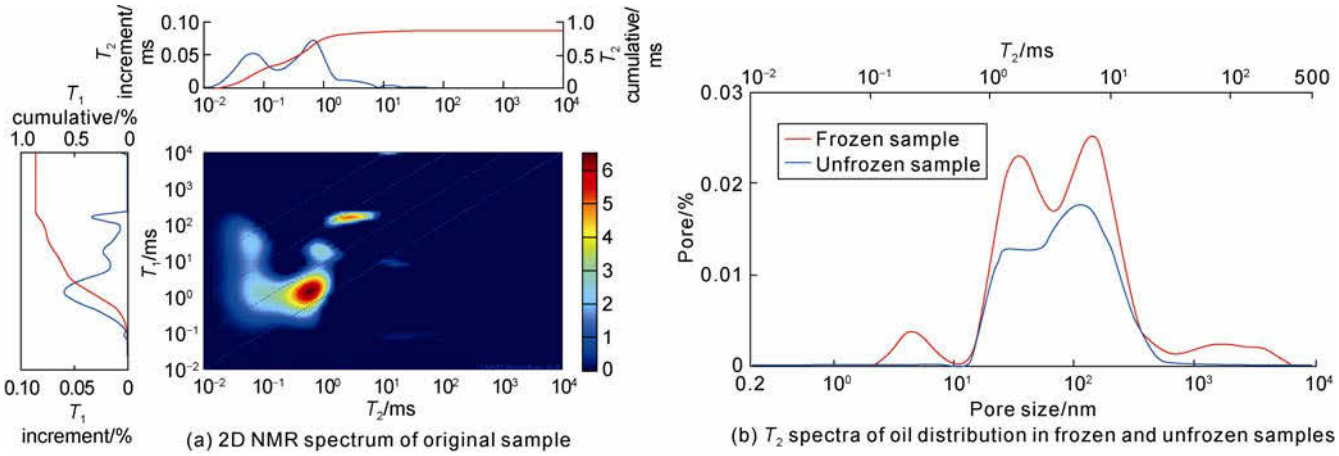

Fig. 11. 2D NMR analysis results of shale samples before and after being naturally unfrozen (Well GY18; 2359.10 m).

is in liquid or gas-liquid state. The results are consistent with theoretical simulation [19], which demonstrates that the phase state of shale oil is affected by nano-confinement effect, characterized by fluid in small pores exhibiting condensate state (or gas state) and fluid in large pores often exhibiting gas-liquid or liquid phase.

The characteristics that pores less than 10 nm generally contain oil and the fact that oil phases vary in different pore sizes indicate that, in the shale oil layer in a Gulong well, even though all oil-bearing pores have similar temperature and pressure, oil in different pores may have different fluid phases and properties. Each oil-bearing pore is a micro- or nano-scale oil accumulation unit with independent fluid phase. It is concluded that Gulong shale oil is composed of numerous micro- and nano-scale oil accumulation units.

7. Conclusions

A large number of pico- and nano-algae are identified in brackish water of the Cretaceous Qingshankou Formation, which are the primary oil precursors in combination with dinoflagellata. The corresponding source rock is characterized by a high hydrogen index and a high hydrocarbon transformation ratio.

Most organic matters in the Qingshankou Formation occur as organo-clay complex. During the matter thermal evolution, clay minerals increase the activation energy, resist kerogen from cracking and extend the oil window. Clay minerals mitigate disproportionation reaction effects on oil cracking by hydrogenation, resulting in more light hydrocarbons.

The formation of accumulation space in Gulong shale

is mainly controlled by dissolution and hydrocarbon generation. At mature stage, dissolution effect on pore formation is significant, while at high mature stage pores formed by hydrocarbon generation is dominant. With diagenetic evolution, micro- and nano-pores decrease, while bedding fractures increase in Gulong shale. Nano-pores and micro-bedding fractures constitute the special dual-porosity media reservoir space in Gulong shale, and provide the important basis for shale oil migration and accumulation.

All-sized pores contain oil, and the visible oil-bearing pore is 5 nm, indicating that Gulong shale oil is generated and accumulated in-situ. Affected by nano-confined effect, shale oil in different-sized pores is in different phases and has different fluidity. It is suggested that Gulong shale oil is composed of a large amount of nano- and micro-scale oil accumulation units.

References

[1] ZHAO Xianzheng, ZHOU Lihong, PU Xiugang, et al. Theories, technologies and practices of lacustrine shale oil exploration and development: A case study of Paleogene Kongdian Formation in Cangdong sag, Bohai Bay Basin, China. Petroleum Exploration and Development, 2022, 49(3): 616–626.

[2] SUN Longde. Gulong shale oil (preface). Petroleum Geology & Oilfield Development in Daqing, 2020, 39(3): 1–7.

[3] SUN Longde, CUI Baowen, ZHU Rukai, et al. Shale oil enrichment evaluation and production law in Gulong Sag, Songliao Basin, NE China. Petroleum Exploration and Development, 2023, 50(3): 441–454.

[4] HE Wenyuan. Discovery and significance of nano pores and nano fractures of clay in Gulong shale oil reservoir in Songliao Basin. Petroleum Geology & Oilfield Development in Daqing, 2022, 41(3): 1–13.

[5] FENG Zihui, LIU Bo, SHAO Hongmei, et al. The diagenesis evolution and accumulating performance of the mud shale in Qingshankou Formation in Gulong area, Songliao Basin. Petroleum Geology & Oilfield Development in Daqing, 2020, 39(3): 72–85.

[6] HE Wenyuan, CUI Baowen, WANG Fenglan, et al. Study on reservoir spaces and oil states of the Cretaceous Qingshankou Formation in Gulong Sag, Songliao Basin. Geological Review, 2022, 68(2): 693–741.

[7] GAO Bo, HE Wenyuan, FENG Zihui, et al. Lithology, physical property, oil-bearing property and their controlling factors of Gulong shale in Songliao Basin. Petroleum Geology & Oilfield Development in Daqing, 2022, 41(3): 68–79.

[8] SUN Longde, LIU He, HE Wenyuan, et al. An analysis of major scientific problems and research paths of Gulong shale oil in Daqing Oilfield, NE China. Petroleum Exploration and Development, 2021, 48(3): 453–463.

[9] ZHU Guowen, WANG Xiaojun, ZHANG Jinyou, et al. Enrichment conditions and favorable zones for exploration and development of continental shale oil in Songliao Basin. Acta Petrolei Sinica, 2023, 44(1): 110–124.

[10] CUI Baowen, ZHAO Ying, ZHANG Ge, et al. Estimation method and application for OOIP of Gulong shale oil in Songliao Basin. Petroleum Geology & Oilfield Development in Daqing, 2022, 41(3): 14–23.

[11] WANG F L, FENG Z H, WANG X, et al. Effect of organic matter, thermal maturity and clay minerals on pore formation and evolution in the Gulong Shale, Songliao Basin, China. Geoenergy Science and Engineering, 2023, 223: 211507.

[12] TISSOT B P, WELTE D H. Petroleum formation and occurrence. 2nd ed. Berlin: Springer, 1984.

[13] ESPITALIÉ J, MADEC M, TISSOT B. Role of mineral matrix in kerogen pyrolysis: Influence on petroleum generation and migration. AAPG Bulletin, 1980, 64(1): 59–66.

[14] HORSFIELD B, DOUGLAS A G. The influence of minerals on the pyrolysis of kerogens. Geochimica et Cosmochimica Acta, 1980, 44(8): 1119–1131.

[15] ZHAO Wenzhi, BIAN Congsheng, LI Yongxin, et al. Enrichment factors of movable hydrocarbons in lacustrine shale oil and exploration potential of shale oil in Gulong Sag, Songliao Basin, NE China. Petroleum Exploration and Development, 2023, 50(3): 455–467.

[16] WANG Y, LIU L F, CHENG H F. Pore structure of Triassic Yanchang mudstone, Ordos Basin: Insights into the impact of solvent extraction on porosity in lacustrine mudstone within the oil window. Journal of Petroleum Science and Engineering, 2020, 195: 107944.

[17] XIN B X, ZHAO X Z, HAO F, et al. Laminae characteristics of lacustrine shales from the Paleogene Kongdian Formation in the Cangdong Sag, Bohai Bay Basin, China: Why do laminated shales have better reservoir physical properties?. International Journal of Coal Geology, 2022, 260: 104056.

[18] ZHANG M M, LI Z. The lithofacies and reservoir characteristics of the fine-grained sedimentary rocks of the Permian Lucaogou Formation at the northern foot of Bogda Mountains, Junggar Basin (NW China). Journal of Petroleum Science and Engineering, 2018, 170: 21–39.

[19] YUAN Shiyi, LEI Zhengdong, LI Junshi, et al. Key theoretical and technical issues and countermeasures for effective development of Gulong shale oil, Daqing Oilfield, NE China. Petroleum Exploration and Development, 2023, 50(3): 562–572.

[20] HE Wenyuan, MENG Qian, FENG Zihui, et al. In-situ accumulation theory and exploration & development practice of Gulong shale oil in Songliao Basin. Acta Petrolei Sinica, 2022, 43(1): 1–14.

[21] HUO Qiuli, ZENG Huasen, QIAO Wanlin, et al. Simulating experiment of hydrous oil generation and expulsion of high-quality source rocks in Songliao Basin. Petroleum

Geology & Oilfield Development in Daqing, 2011, 30(2): 1–5.

[22] FENG Zihui, HUO Qiuli, ZENG Huasen, et al. Organic matter compositions and organic pore evolution in Gulong shale of Songliao Basin. Petroleum Geology & Oilfield Development in Daqing, 2021, 40(5): 40–55.

[23] YUAN Chao, XU Qinzeng, SHAO Hebin, et al. Distribution of picophytoplankton from subtropical pacific to Chukchi Sea during late summer. Advances in Marine Science, 2021, 39(3): 430–440.

[24] KRIENITZ L, BOCK C, KOTUT K, et al. *Picocystis salinarum* (Chlorophyta) in saline lakes and hot springs of East Africa. Phycologia, 2012, 51(1): 22–32.

[25] FENG Zihui, FANG Wei, WANG Xue, et al. Microfossils and molecular records in oil shales of the Songliao Basin and implications for paleo-depositional environment. Science China Earth Sciences, 2009, 52(10): 1559–1571.

[26] CAI Jingong. Organo-clay complexes in muddy sediments and rocks. Beijing: Science Press, 2004: 53–143.

[27] CHEN Z H, LIU X J, JIANG C Q. Quick evaluation of source rock kerogen kinetics using hydrocarbon pyrograms from regular Rock-Eval analysis. Energy & Fuels, 2017, 31(2): 1832–1841.

[28] PAN C C, JIANG L L, LIU J Z, et al. The effects of calcite and montmorillonite on oil cracking in confined pyrolysis experiments. Organic Geochemistry, 2010, 41(7): 611–626.

[29] YANG S Y, HORSFIELD B. Some predicted effects of minerals on the generation of petroleum in nature. Energy & Fuels, 2016, 30(8): 6677–6687.

[30] SHAO Hongmei, GAO Bo, PAN Huifang, et al. Diagenesis-pore evolution for Gulong shale in Songliao Basin. Petroleum Geology & Oilfield Development in Daqing, 2021, 40(5): 56–67.

[31] LOUCKS R G, REED R M, RUPPEL S C, et al. Spectrum of pore types and networks in mudrocks and a descriptive classification for matrix-related mudrock pores. AAPG Bulletin, 2012, 96(6): 1071–1098.

[32] MILLIKEN K L, RUDNICKI M, AWWILLER D N, et al. Organic matter–hosted pore system, Marcellus Formation (Devonian), Pennsylvania. AAPG Bulletin, 2013, 97(2): 177–200.

[33] SUN L D, HE W Y, FENG Z H, et al. Shale oil and gas generation process and pore fracture system evolution mechanisms of the continental Gulong Shale, Songliao Basin, China. Energy & Fuels, 2022, 36(13): 6893–6905.

[34] BARTH T, BJØRLYKKE K. Organic acids from source rock maturation: Generation potentials, transport mechanisms and relevance for mineral diagenesis. Applied Geochemistry, 1993, 8(4): 325–337.

[35] YANG Zhi, ZOU Caineng, WU Songtao, et al. Characteristics of nano-sized pore-throat in unconventional tight reservoir rocks and its scientific value. Journal of Shenzhen University (Science & Engineering), 2015, 32(3): 257–265.

[36] ZOU Caineng, ZHU Rukai, BAI Bin, et al. First discovery of nano-pore throat in oil and gas reservoir in China and its scientific value. Acta Petrologica Sinica, 2011, 27(6): 1857–1864.

[37] KHATIBI S, OSTADHASSAN M, XIE Z H, et al. NMR relaxometry a new approach to detect geochemical properties of organic matter in tight shales. Fuel, 2019, 235: 167–177.

[38] LI Haibo, ZHU Juyi, GUO Hekun. Methods for calculating pore radius distribution in rock from NMR T_2 spectra. Chinese Journal of Magnetic Resonance, 2008, 25(2): 273–280.

[39] SONG Z J, SONG Y L, GUO J, et al. Effect of nanopore confinement on fluid phase behavior and production performance in shale oil reservoir. Industrial & Engineering Chemistry Research, 2021, 60(3): 1463–1472.